Beams-doc-5816

Study of Microchannel Plates as a Novel Approach to Electron Gun Design for Electron Lenses

Magnus Haughey [1, 2, 3]

August, 2017

1. School of Physics and Astronomy, University of Edinburgh, Edinburgh, UK.
2. Summer intern at Fermilab, Batavia, IL, under supervision of V. Shiltsev and G. Stancari
3. s1332744@sms.ed.ac.uk

Abstract

A recent proposal suggested the use of microchannel plates as cathodes for electron guns, as part of a novel electron lens design to be tested in the IOTA facility at Fermilab National Laboratory, Batavia, IL. To assess the suitability of microchannel plate technology in this design, a study of microchannel plate based photomultiplier (MCP-PMT) systems is performed. A systematic study of the Burle 85011-501 MCP-PMT is presented, including results from time response tests and maximum current density tests using different sources of light pulses. An investigation into the effects of magnetic fields on the MCP-PMT properties is also carried out. The Burle 85011-501 is shown to have good time response properties — being capable of producing nanosecond order responses — however maximum current values drawn from the device do not reach the desired value for the new electron lens design. The device performance is shown to have a strong dependency on magnetic field strength. Suggested work and improvements for future studies are suggested.

Introduction

Space charge (SC) effects in charged particle beams can be a major source of beam loss and instabilities. These effects, which arise from electromagnetic interactions of individual particles with the charged particle beam, become dominant for particle beams with lower β factors, and so addressing these effects in lower energy machines and in proton beams is crucial. One of the many facets of accelerator research and development concerns technology designed to compensate for these effects.

This report is centered around the proposal of using a microchannel plate (MCP) as the cathode of an electron gun, in a new electron lens design. A study of an MCP based photomultiplier (PMT) device is conducted with the aim of characterizing MCP technology. A comprehensive understanding of MCPs is required in order to assess their suitability as cathodes of an electron gun. Details of the proposal can be found in section entitled “MCP Electron Gun”.

FAST/IOTA

The development of technology to be used for space-charge compensation will be one of the focuses of the Fermilab Accelerator Science and Technology (FAST) facility at Fermilab

National Laboratory, Batavia, IL. This facility hosts the Integrable Optics Test Accelerator (IOTA) [1], a 40 meter diameter storage ring which will be used for accelerator research and development. With the first commissioning of the accelerator with electron beams forecast for 2018, IOTA will utilize new and state-of-the-art technologies in both the test ring itself and in the two 130 meter long linacs. In the existing linac [2], electron bunches are generated by illuminating a photocathode with frequency quadrupled UV light ($\lambda = 263\mu m$) and are accelerated to a nominal energy of 150 MeV. This injector is similar in design to the linac proposed for the ILC electron-positron collider and utilizes an ILC-type cryomodule housing eight superconducting radio-frequency cavities. The second linac is the proposed proton injector which will generate 2.5 MeV proton bunches and inject them into the ring at a frequency of 325 MHz. IOTA will facilitate an array of innovative experiments in beam dynamics by virtue of the flexibility of the lattice and its capability of maintaining stable beam over a range of beam sizes.

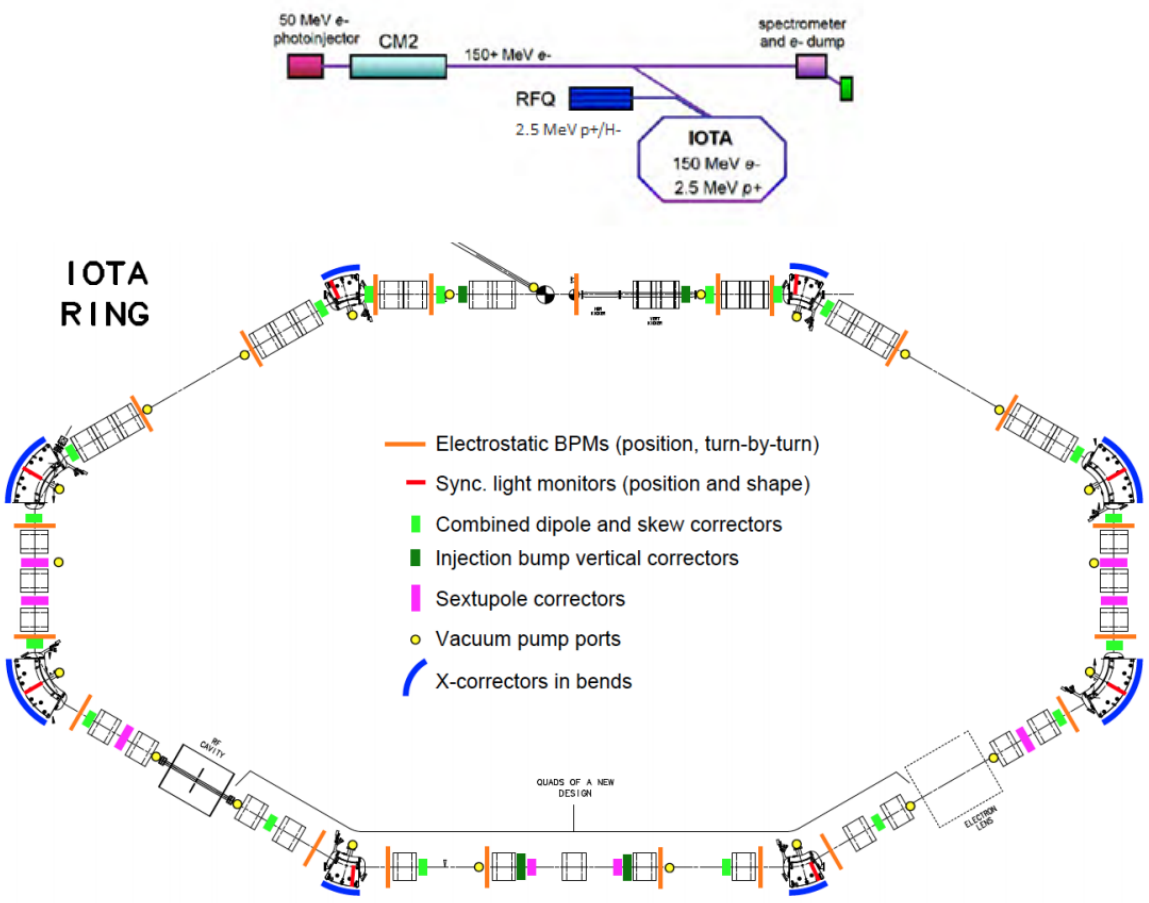

Figure 1: **(Top)** Schematic of the FAST/IOTA injector, showing single ILC-type cryomodule currently installed. **(Bottom)** Layout of the IOTA storage ring, indicating the positions of main magnets and beam diagnostic apparatus around the 40 m diameter. The electron lens position is indicated by the grey box in the lower right section of the ring.

Space Charge Effects

Space charge effects in charged particle beams lead to a number of unwanted phenomena, including particle loss, emittance growth and beam instabilities. These effects derive from

the self-fields of the particle beam. Individual particles in the beam experience a repulsive force from the electric field generated by the charged beam and an attractive magnetic force due to translation parallel to the other charged particles. The overall radial force on the particle is proportional to the charge distribution, λ, and Lorentz factor, γ, of the beam:

$$F_r(r) \propto \frac{\lambda}{\gamma^2} \tag{1}$$

The inverse-square dependence of the radial space charge force on the Lorentz factor indicates that these effects are more pronounced in proton beams. Moreover, as depicted in Fig. 2, the space charge forces are non-linear and cannot be countered by regular quadrupole magnets.

A method to compensate for space charge forces in high energy proton beams is to

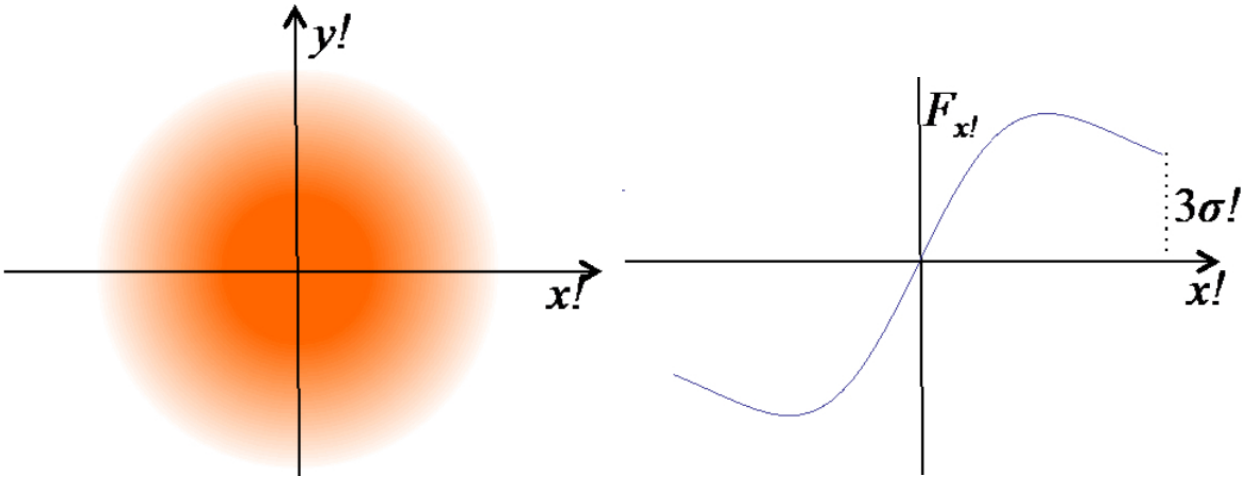

Figure 2: Plot of one-dimensional space charge forces (radial) for a beam with Gaussian transverse distribution. Force is linear at small radii and develops a $1/r$ dependence at larger values of r. Image from Ref. [3].

generate an electron beam which is magnetically confined to circulate with the protons over a small fraction of the accelerator circumference [4]. In order for these so-called electron lenses to supply the non-linear focusing to the proton beam and provide full compensation for space charge effects, they must satisfy several requirements. Firstly, they must generate electrons with a transverse distribution which matches that of the circulating protons. Additionally, the longitudinal profile of the electrons must be generated with precise timing and allow for matching of space charge forces along the longitudinal direction. Also, for full compensation of space charge forces, the electron lens must be designed to compensate over a small length for the defocussing that takes place around the entirety of the circumference of the ring [5].

A common design for existing electron guns utilizes thermionic cathodes to generate electrons. These are devices, made from materials chosen from their low work function and high quantum efficiency properties, which are heated to temperatures of around 1000°C such that they produce electrons by thermionic emission. The electrons are bunched and accelerated by pulsing an anode from a negative potential to ground over timescales of 100 ns. These designs have been used for previous electron lenses, for example in Tevatron, Fermilab [6], however they are limited by the timescale associated with pulsing the anode, and so to attain full space charge compensation remains a major challenge.

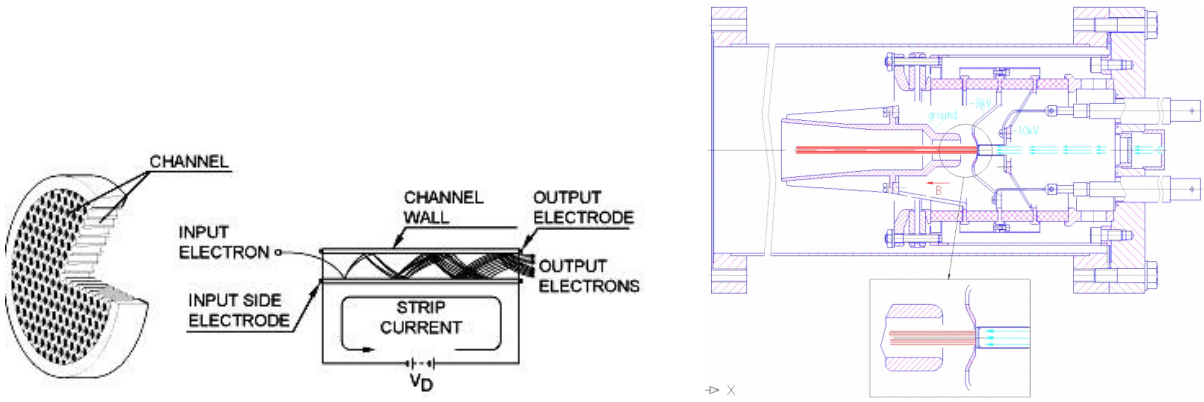

Figure 3: (Left) Schematic of MCP plate, showing details of individual channels within. **(Right)** Layout of DC electron gun with an MCP cathode. Magnified section depicts laser light (blue arrows) illuminating MCP cathode from the right, and the output stream of electrons (red) traveling out from the MCP (see Ref. [7]).

MCP Electron Gun

The central concept behind this study is the proposal to use an MCP as the cathode of an electron gun, with the view of incorporating this new design into electron lenses for IOTA and in other active experiments, such as the LHC in Geneva, Switzerland. As shown in Fig. 3, microchannel plates consist of millions of glass capillaries, which are fused together and sliced into O(mm) thick plates. Each face of the MCP is coated with electrode material, to which high voltage of 1—2 kV is applied. When in operation, each of the semiconducting capillaries act as independent electron multipliers. Incoming radiation entering the channels, such as electrons, neutrons or UV/X-ray photons, will release secondary electrons which are accelerated towards the end of the channel. Along these trajectories, the electrons will repeatedly collide with the channel walls, each causing more secondary electrons to be released. The electron avalanche which follows results in thousands of electrons exiting the MCP. Typical gain values for MCP devices are of the order O(10^3) for a single plate and O(10^6) for two stacked MCPs. These devices operate comfortably at room temperatures, under vacuum of the order O(10^{-7} Torr).

To use an MCP as the cathode of an electron gun would bring several marked benefits over previous thermionic cathode designs [7]. The ability of MCP devices to operate at room temperature allow for improvements to the mechanical stability of the electron gun system, as well as improved vacuum conditions. This may also lead to a reduced emittance (6-dimensional volume in position-momentum phase space) of the resultant electron beam. MCP devices can have a quantum efficiency of around 15–30%, which is a tenfold improvement on other electron gun designs that use photosensitive materials, such as photoinjectors. MCPs are an also attractive option for the design of an electron lens due to their fast timing properties [8]. These technologies possess a superior pulse width — or spread in transit time of electrons — to the traditional dynode based PMTs due to the small diameter of the MCP channels, giving rise to a smaller spread in individual trajectories [9]. As mentioned previously, the typical timescale on which traditional modulated anode electron guns operate is 100 ns, and so response times of in the order of nanoseconds which are associated with MCP-PMT devices will bring major advantages to the new design. The MCP electron gun design would also offer a simplified layout in comparison to traditional electron gun designs, as can be seen in Fig. 3, in which the MCP is illuminated by the laser from behind.

Experimental Results

A systematic study of MCP-based photomultiplier devices (referred to as MCP-PMTs herein) is performed with the aim of characterizing MCPs and assessing their suitability in the design outlined in the previous section. As depicted in Fig. 4, the MPC-PMT devices used in this study consist of a photocathode, MCP, and anode/readout electronics. Two

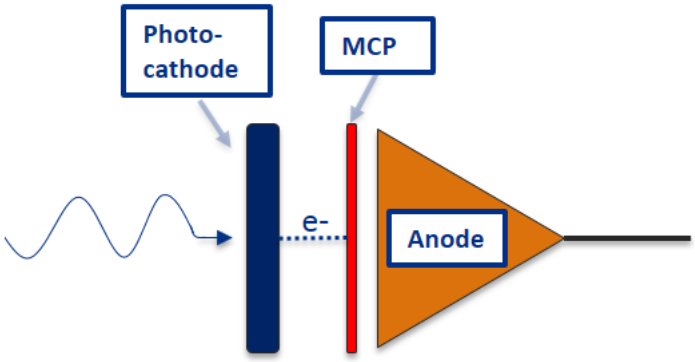

Figure 4: Layout of typical MCP-PMT device showing, from left to right: incoming radiation; photocathode; photoelectron (dashed blue track); MCP; anode & readout.

main stages of experiment are performed: tests using flashing LEDs and a pulsed laser. Throughout the study, two main properties of the MCP-PMT are investigated: the maximum current density achievable, and the shortest signal width. To achieve a current density of around 1 Acm^{-2} would give a good indication that the MCP technology is suitable for the electron lens design. This is because such a value of current density will correspond to an electron bunch that will generate a strong enough electric field to provide space charge compensation in the IOTA proton beam. With a current density of this order of magnitude, magnetic compression techniques can then be utilized to match the current density at the cathode to the desired value inside the electron lens. The timing properties of the MCP-PMT are also important, and an output signal with a width of the order of nanoseconds will, again, give a good indication that the technology is capable of performing in the electron lens. This goal is considered according to the IOTA bunch length, 3 ns. In addition to these two quantities, the effects of immersing the MCP-PMTs in a magnetic field are also explored. Each of these factors will help to determine if an MCP cathode is a viable option in new electron lens designs. Details of the MCP-PMT device used throughout this study are presented, followed by results from the LED and laser tests.

Burle 85011-501 MCP-PMT

The MCP-PMT device used throughout this study is the Burle 85011-501 MCP-PMT [10]. It is a two-stage device, using two MCPs in the electron-multiplying stage to provide a typical gain value of 7×10^5 at an applied voltage of -2.5 kV. This MCP-PMT has 64 channels, or discrete pixels, which can be individually read out as a voltage signal. It is capable of a time response of around 300 picoseconds, and the bialkali photocathode is sensitive to

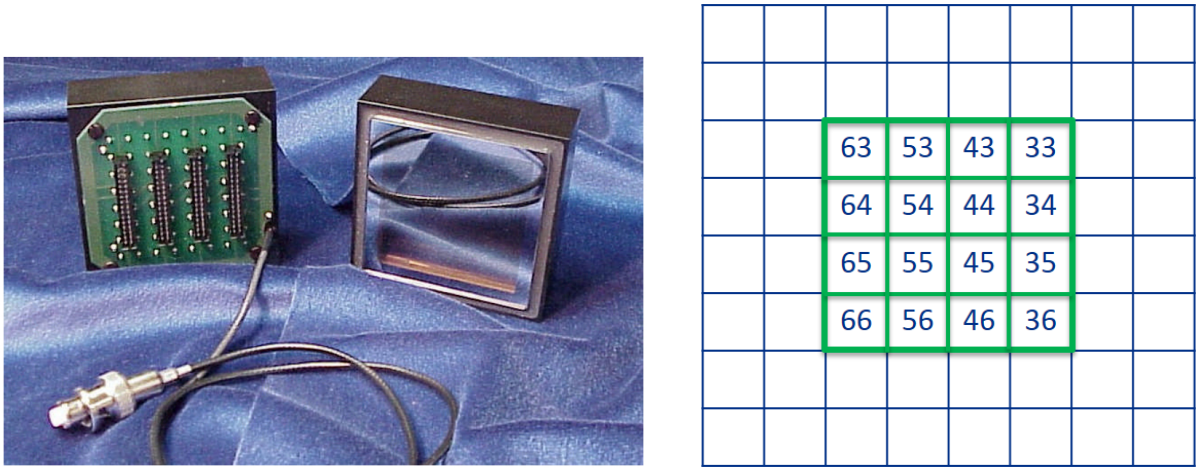

Figure 5: (Left) Back and front view of Burle 85011-501 MCP-PMT, showing high voltage cable (Image from Ref. [10]). **(Right)** Diagram of 8x8 matrix of pixels on the face of the MCP-PMT. Anodes for the channels outlined in green are connected to readout cables, with the numbers denoting channel number. Channels outlined in blue with no numbers are inactive (not connected to readout cables).

wavelengths in the visible region from 185 to 660 nanometers, with a peak sensitivity at 400 nanometers. Fig. 5 shows two views of the MCP-PMT device, and a diagram of the channels on the front face.

LED Experiments

A simple, desk-top setup is used for the LED tests. Fig. 6 depicts such an arrangement, showing the function generator which is used to send pulses of current to a blue LED inside a dark box. Also mounted in the box is the Burle MCP-PMT, powered by a high voltage (HV) power supply, from which the signals are read out on an oscilloscope, also shown. To perform studies of this system, the blue LED is flashed using the function generator, illuminating the face of the MCP-PMT. The voltage supplied to the MCP-PMT can be varied, as well as the form of the LED pulses which is controlled using the function generator.

The first study performed is a simple exploration of the shortest pulse which can be read out by the MCP-PMT. Fig. 6 shows a typical scope readout from these tests. Peak widths of around 50 nanoseconds can be achieved. This system appears to be limited by the capabilities of the function generator and the LED, however, since reducing the pulse width in the LED below 50 nanoseconds leads to a reduction in voltage amplitude to the LED. As such, no more consideration is given to peak width (see, however, section entitled "Laser Experiments" for further discussion on pulse width).

In addition to the minimum pulse width, other aspects of the MCP-PMT are characterized. Two dependencies are focused on, these being the relationship of MCP-PMT output amplitude with 1. voltage applied to MCP-PMT device and 2. duty factor, defined as the ratio of the pulse width and the pulse period from the light source. Fig. 7 shows data from such experiments. The manufacturer recommendation for applied voltage is -2.6 kV [10], however to preserve the lifetime of this particular device, the applied voltage does not exceed -2.4 kV on any occasion. The MCP-PMT output amplitude appears to have a non-linear dependence on the applied voltage. This is in disagreement with similar data obtained using

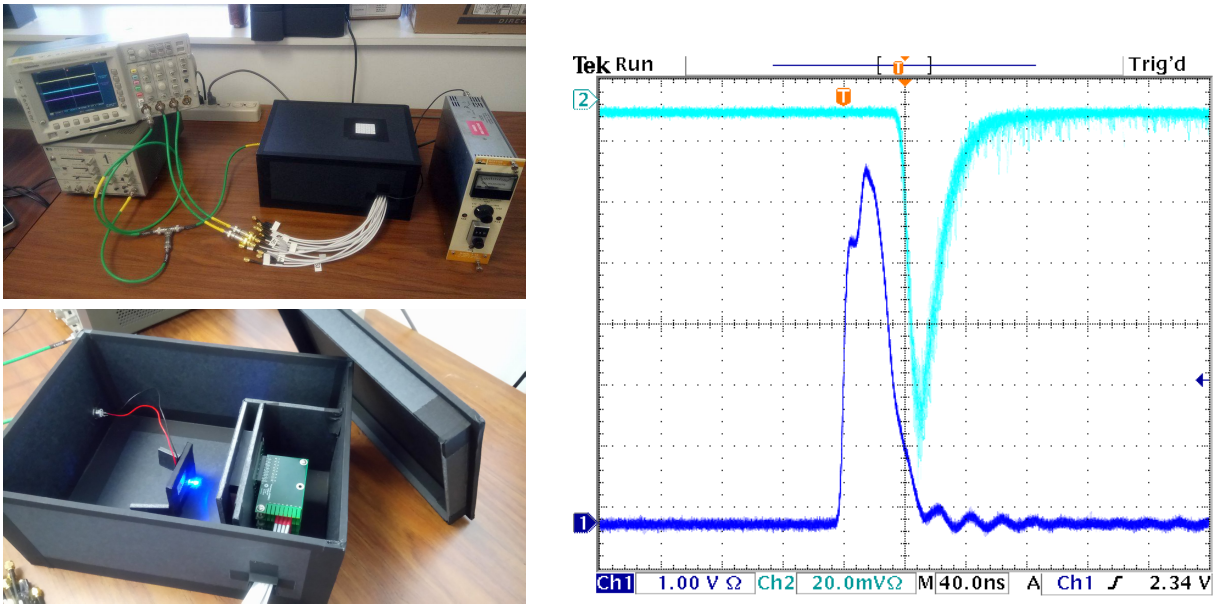

Figure 6: (Left) Upper image shows the desk-top setup for LED experiments. Pulses of voltage generated by function generator, bottom left, which power the LED contained inside the black box. Also inside the dark box is the MCP-PMT, with white readout cables connected to oscilloscope. High voltage power supply, right, powers the MCP-PMT. Lower image shows inside of the dark-box, with the blue LED illuminating the face of the MCP-PMT. **(Right)** Typical scope readout for flashing blue LED system. Dark blue trace is signal from the function generator, which is connected to the blue LED. Cyan trace is output signal from MCP-PMT, channel 44 (see Fig. 5). 40 ns/div. Measured with a Tektronix oscilloscope (TDS3034B, 300 MHz, 2.5 GS/s)

a pulsed laser which is believed to be more accurate (see section entitled "LASER Experiments"). From the data in Fig. 7, the maximum output amplitude attainable is around 650 mV. After calculating the corresponding current (considering the 50 ohm load of the oscilloscope), and dividing by the area of one pixel in the MCP-PMT device, the corresponding current density is around 32 $mAcm^{-2}$. This is one twentieth of the desired current density. This value seems to be limited by the irradiance and pulse width of the LED. A higher intensity light pulse with larger average power could perhaps lead to significant increases in current density. The dependence of MCP-PMT output amplitude on duty factor is explored by varying the frequency of LED pulses, keeping the pulse width constant. A relatively small range of frequency values is studied, due to limitations imposed by the function generator, yet a strong dependence on the duty factor is observed and is demonstrated for two channels of the MCP-PMT in Fig. 7. Even at a frequency value of 1 kHz, corresponding to a duty factor value of $5x10^{-3}$ % for pulse width of 50 ns, the MCP-PMT signal is heavily suppressed in comparison the signal at 100 Hz. The reasons for this are unknown, however on page 285 in Ref. [8] the author describes briefly that when MCP-PMT devices are operated at high voltages, the resulting gain may be large enough that the charge at the back face of the plate (at the channel exits) limits the total charge per pulse. The observations from the duty factor experiments in this study may be a demonstration of this effect: if the charge at the back plate of the MCP cannot dissipate quickly enough then as the duty factor increases there may be a build up of space charge, limiting the total output charge of the pulses. It will be crucial to consider this effect when assessing the suitability of MCP technology for the electron gun design.

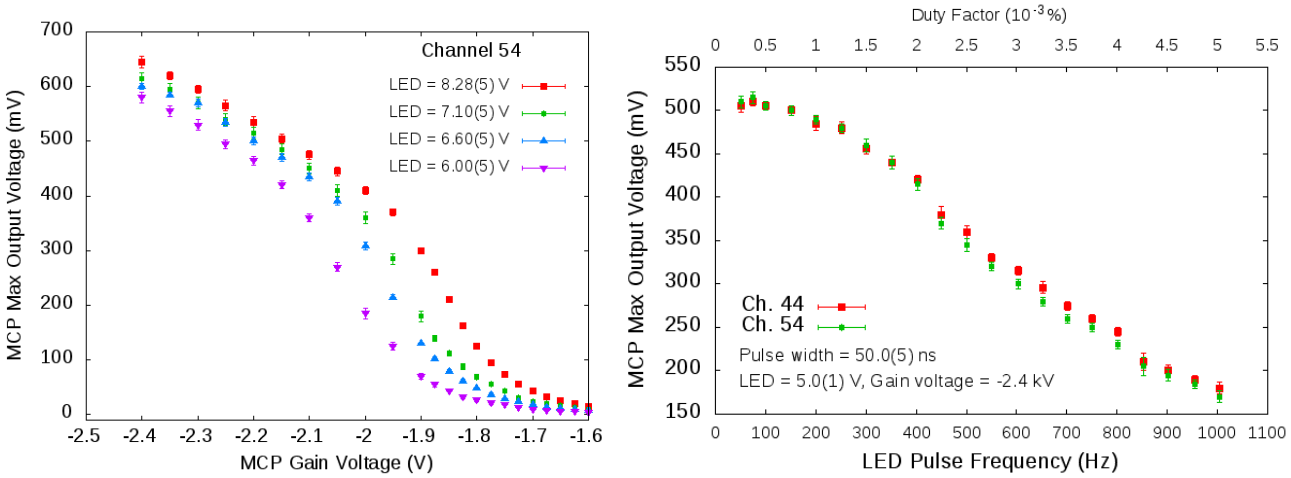

Figure 7: Data from LED tests. **(Left)** MCP output amplitude versus applied gain voltage, MCP-PMT channel 54. Four different colored data sets correspond to different peak voltages applied to the blue LED. **(Right)** MCP output amplitude versus duty factor for MCP-PMT channels 44 (red) and 54 (green).

Laser Experiments

The second stage of this study concerns tests using a 635 nm pulsed laser. Fig. 8 shows the set up of these experiments, in which the same Burle MCP-PMT is used. This laser

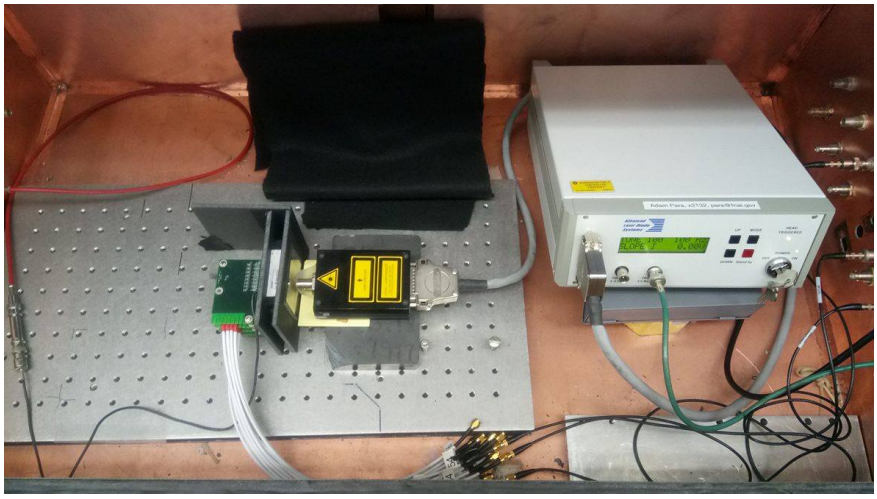

Figure 8: Experimental setup for laser tests, showing the MCP-PMT device (left), laser head (middle) and laser controller (right). Aparatus is situated inside a light-tight box.

is much faster than the LED system, and as such the shortest achievable pulse from the MCP-PMT is in the region of 5 ns — similar to the IOTA bunch length, 3 ns. Fig. 9 shows a typical scope readout from the laser tests, demonstrating such a pulse from the MCP-PMT. The outcome of a study into the relationship between the MCP-PMT response time with frequency are also presented. These results suggest a relationship between these two quantities, with the response time roughly increasing logarithmically with frequency. It should be noted that the data corresponding to larger frequency values are less reliable. The reason for this is that at these values of frequency, the duty factor is large enough to suppress the MCP-PMT response, reducing the resolution of the signal on the scope. For this reason,

its response time at frequencies relevant to IOTA (∼8 MHz) are not explored. The fact, however, that the MCP-PMT appears to perform more poorly at higher frequencies will be an important factor in designing the MCP-based electron gun, and this relationship should be characterized more fully for a range of MCP devices in future studies. In addition to this, the response from the MCP-PMT appears to be not entirely smooth (as can be seen in the cyan scope trace in Fig. 9). This may be due to reflections in the cables and so perhaps cannot be attributed to the MCP within the MCP-PMT device. Another possible origin of this effect however, which does occur in the electron multiplying stage of the MCP-PMT, is the phenomenon of afterpulses [11]. This describes the effect of a late pulse of electrons arising at the anode, partly due to ionisation of residual gases inside the detector, which are accelerated in the opposite direction to the electrons yet may give rise to further secondary electron emission when they collide with the channel wall. This effect, however, is widely understood and one would not expect to observe afterpulses of this nature until several hundreds of nanoseconds after the main pulse [12]. Further, the control of this effect is addressed in the design of MCP-PMT devices with the bias angle[1]. The observation of small secondary peaks in this system however must be characterized and understood when designing the MCP-based electron gun.

Studies of the effects of applied gain voltage and varying duty factor are also performed

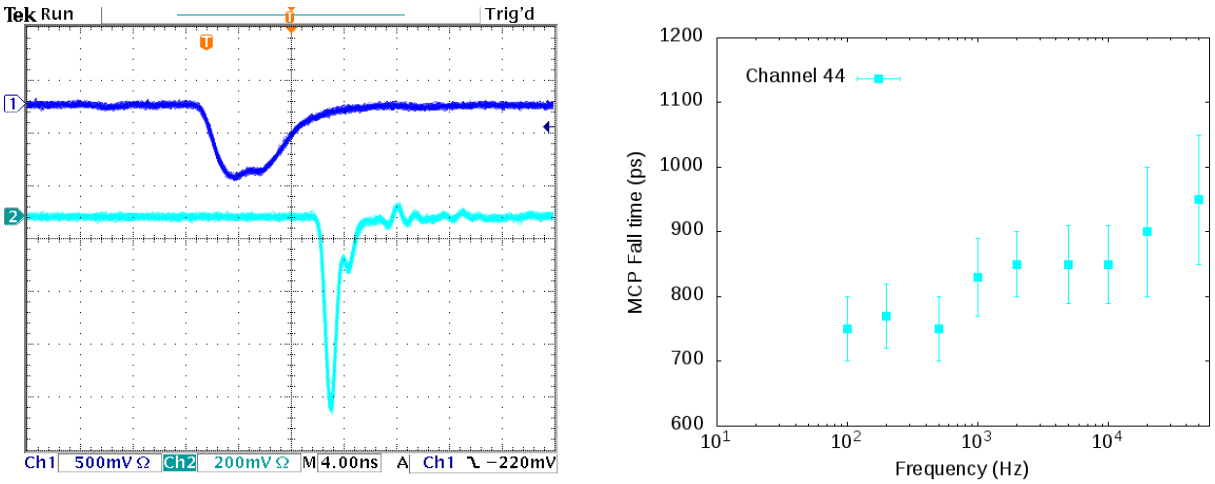

Figure 9: (Left) Typical scope readout for laser test. Dark blue trace is signal from the laser controller, and so corresponds to the laser pulse. Cyan trace is output signal from MCP-PMT, channel 44 (see Fig. 5). 4 ns/div. Measured with a Tektronix oscilloscope (TDS3054B, 500 MHz, 5 GS/s) **(Right)** MCP-PMT Fall resonse time (fall time) versus laser frequency. Logratithmic scale in the horizontal axis.

with the laser system. It is possible to obtain more informative data with the laser than with the LED since an element of human error (associated with operating the pulse generator) is eliminated in the laser system. Moreover, the capabilities of the laser are such that it can produce shorter pulses than the LED, and a greater range of frequencies can be explored (up to 1 MHz). Fig. 10 shows data from these studies. The results from both studies differ somewhat from the corresponding data from the LED studies. A linear relationship between MCP-PMT output amplitude and applied MCP-PMT voltage is observed between -2.4 kV and -2.0 kV. This is also observed in the LED data, however the functional form of

[1]Microchannel plates are designed to minimise secondary electron production by positive ions by choosing the axis of the channels to make a small angle with the normal axis of the plate itself. This angle, termed the *bias angle*, is usually around 8° to 15° and is chosen such that the positive ions can not be accelerated to energies sufficient to create secondary electrons before they collide with the channel wall.

the data differs between -2.0 kV and -1.6 kV. Despite the pulse width of the laser being an order of magnitude smaller than those produced by the LED, the maximum voltage output from the MCP-PMT is still small — just under 400 mV as can be seen from Fig. 10. As with the LED tests, this value corresponds to around one twentieth of the desired value of 1 Acm^{-2}. Brief tests using a laser with a greater peak power show that this value can be increased (magnetic field tests, addressed in a later section, are conducted using a laser with a marginally higher peak power and lead to peak current densities in the region of 60 Acm^{-2}). This suggests that an upper limit on the current density available from this particular MCP-PMT device has not yet been established, and more powerful lasers should be considered in future tests. Note again, however, the comments made on page 285 in Ref. [8] regarding the possible upper limit on the total charge available per pulse in microchannel plate-based devices (between 10^6 and 10^7 electrons). This statement should be challenged with further testing of MCP-PMT devices, to understand if it holds even at the very low values of duty factor. One objective for this study was to utilize the laser used in the FAST injector. Due to technical constraints, however, this has not been possible.

A far greater range of frequencies, and therefore duty factors, can be explored with the laser. The frequency of the laser is varied from 100 Hz to 1 MHz, spanning four orders of magnitude in the duty factor. The data from these tests support those from the LED tests, showing increases in the duty factor to have a strong negative effect on the peak output voltage from the MCP-PMT. More is revealed about the relationship between the output voltage and the duty factor with these tests, and it is observed that the output voltage increases exponentially with decreasing duty factor over the range [100 Hz : 1 MHz]. Or, conversely, the output signal from the MCP-PMT is nearly zero at 1 MHz.

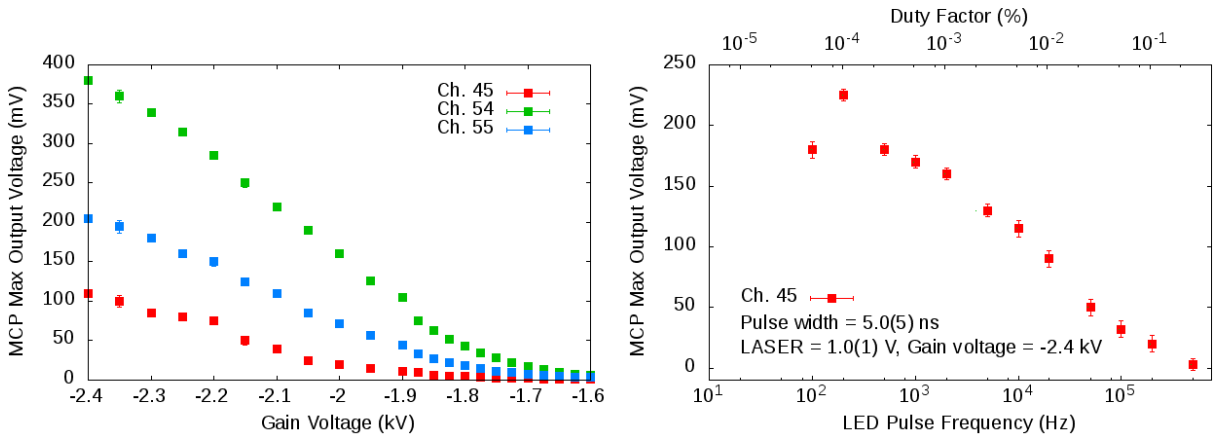

Figure 10: (Left) MCP-PMT output amplitude versus applied gain voltage. Three colors of data points correspond to different MCP-PMT channels.**(Right)** MCP-PMT output amplitude versus duty factor. Logarithmic scale in the horizontal axis.

In addition to the aforementioned studies carried out with the laser system, the effects of a magnetic field is also explored. The working electron gun, and electron lens, must operate in a solenoidal magnetic field, and so to characterize its effect on the performance of MCP-PMT devices is important. A permanent magnet is used, with maximum fields strength of $\sim$ 700 G (typical magnetic field strengths are between 2 kG and 4 kG). The aperture of the magnet is not large enough to accommodate the MCP-PMT and laser, and so the experiments are conducted using the fringes of the field. The magnetic field strength in the volume occupied by the MCP-PMT is controlled by varying the distance

of the device from the magnet aperture in both cases. The magnet, and experimental setup are shown in Fig. 11. Due to time constraints of this study, only two configurations are explored: 1. Magnetic field perpendicular to the MCP channels (see Fig. 3) and 2. Magnetic field and MCP channels parallel. The latter is of particular interest, as this recreates more accurately the configuration of the electron lens. Measurements of MCP-PMT output amplitude versus magnetic field strength are presented in Fig. 12, showing data corresponding to both configurations. A strong dependency is observed in both scenarios — with the MCP-PMT device performing poorly even in a relatively weak magnetic field. One MCP-PMT channel is studied in the perpendicular configuration, the results for which show a linear decay in MPC-PMT output amplitude with magnetic field strength. This particular result is in agreement with the work of D. Beznosko [13] who also found a similar stark decrease in performance quality of the Burle 85011-501 MCP-PMT in magnetic fields. For the parallel configuration, two MCP-PMT channels are studied. The data from the parallel configuration, despite only a few points, also hint at a negative impact on the MCP-PMT performance with increasing magnetic field strength. This is likely due to the electrons being accelerated by the magnetic field back to the walls of the channel before they have sufficient energy to cause more electron emission. An interesting case, which should be pursued in future studies, would be to observe the performance of the MCP-PMT device when the field is strong enough such that the Larmor radius of the electrons within the MCP is smaller than the radius of the channel. In this system, the electrons will still follow a curved trajectory due to any transverse velocity with respect to the magnetic field lines, however the radius of this curve may be small enough prevent them from immediately colliding with the channel walls. If this is the case, one may observe the output voltage return to values in the same order as those in the zero field.

For future magnetic field experiments, more precise measurements should be taken. The experiments performed in this study utilize the fringe-field of a permanent magnet, which is highly non uniform throughout the volume of the MCP-PMT device. To use a solenoid or a similar device will allow for a more uniform magnetic field, and would better recreate the field which will be present in the electron lens itself. This will provide greater insight into how MCP devices will perform in electron lenses, and should allow for greater precision when arranging the MCP-PMT device — something which proves challenging with the current experimental setup.

Conclusions and Future Work

A systematic study of an microchannel plate based photomultiplier device has been carried out. One particular device, the Burle 85011-501 MCP-PMT, is used throughout the project. Characterization of MCP-PMT technology is performed with the intention of understanding if and how an MCP can be incorporated into a new electron gun design for electron lenses in IOTA. Experiments using flashing LED and pulsed laser are performed with the aim of exploring the shortest pulse which can be read out from the MCP-PMT, and the maximum current density which can be drawn from the device. These aims have been formulated by considering the properties of the IOTA ring and the necessary functions of an electron lens. Studies of the MCP-PMT performance are reported, with results from tests in which the voltage supplied to the MCP-PMT is varied, and for varying duty cycle of light pulses. A linear relation between output amplitude from the device and applied voltage is observed in the region around the nominal operating voltage for both LED and laser tests. Exponential decrease in output amplitude from the MCP-PMT with increasing duty factor

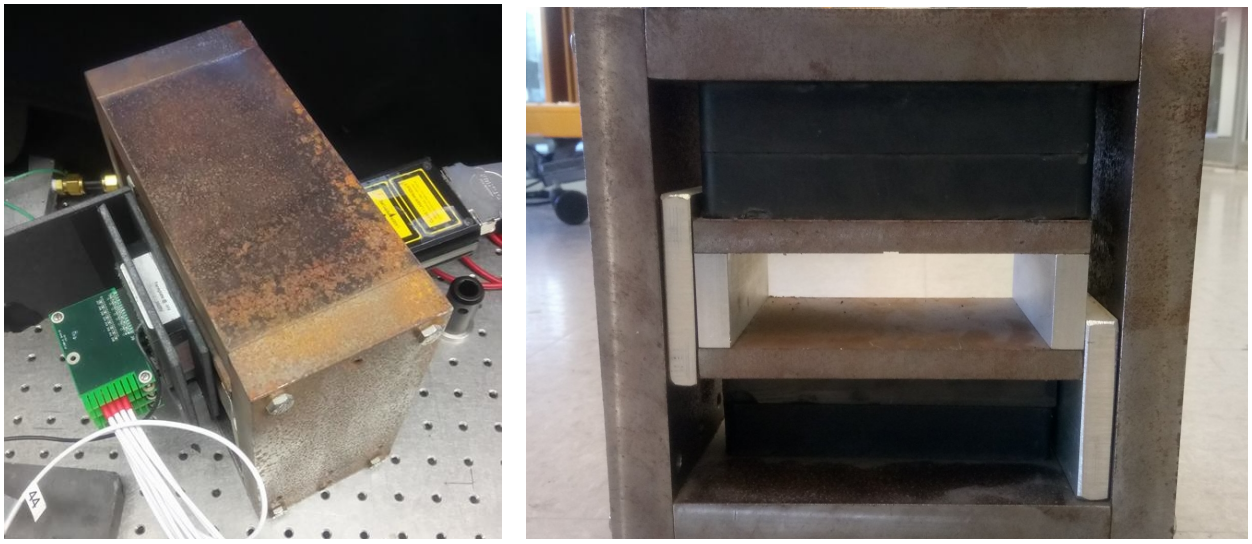

Figure 11: (Left) Experimental setup for magnetic field tests. Image shows Burle MCP-PMT device, left, with front plate facing into the magnet aperture. Laser can be seen on the right side of the image, with the beam pointing through the magnet apertude onto the MCP-PMT face. **(Right)** Front view of the permanent magnet used for magnetic field tests.

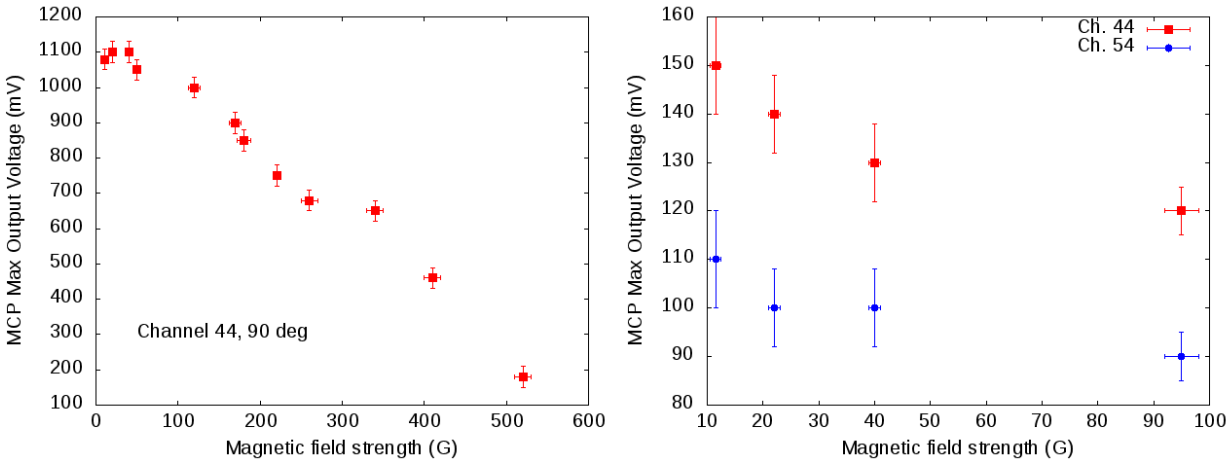

Figure 12: MCP-PMT output amplitude versus magnetic field strength for: **(left)** perpendicular configuration; **(right)** parallel configuration.

is observed for the laser tests. The MCP-PMT device shows good time response properties, with output signal peaks around 5 ns in width achieved in the laser tests. The goal of obtaining a current density in the region of 1 Acm^{-2} has not been achieved. Suggestions for continuing this endeavor are suggested, including the use of the FAST laser. Additionally, a major dependence of MCP performance on magnetic field strength is reported, for magnetic field parallel and perpendicular to axis of the MCP channels. Directions for future work are suggested: the most significant of which being to use shorter and more intense laser pulses to obtain a larger output amplitude from the MCP-PMT, and to make more precise magnetic field measurements over a larger range of field strengths. The lifetime of the MCP-PMT devices should also be considered in future studies, since the use of these devices for such purposes as obtaining high output current may shorten the length of time over which they perform reliably.

References

[1] S. Antipov, S. Nagaitsev, and A. Valishev, Journal of Instrumentation **12**, P04008 (2017).

[2] P. Piot et al., The advanced superconducting test accelerator (asta) at fermilab: A user-driven facility dedicated to accelerator science and technology, 2013.

[3] M. Ferrario, M. Migliorati, and L. Palumbo, Space Charge Effects, 2016.

[4] G. Stancari et al., Electron lens for the fermilab integrable optics test accelerator, in *Proceedings of the 57th ICFA Advanced Beam Dynamics Workshop on High-Intensity and High-Brightness Hadron Beams*, 2016.

[5] V. Shiltsev, *Electron Lenses for Super-Colliders*, Springer, New York, NY, 2016.

[6] V. Shiltsev et al., Physical Review Special Topics Accelerators and Beams **11**, 103501 (2008).

[7] V. Shiltsev, New possibilities for beam-beam and space-charge compensation: Mcp gun and electron columns, in *2007 IEEE Particle Accelerator Conference (PAC)*, pages 1159–1160, 2007.

[8] G. F. Knoll, *Radiation detection and measurement*, Wiley New York, 2nd ed. edition, 1989.

[9] J. S. Milnes and J. R. Howorth, Proc. SPIE **5580**, 730 (2005).

[10] Planacon^{TM} Photomultiplier Tube Assembly 85011-501, `https://psec.uchicago.edu/library/MCP_info/data_sheet_85011-501.pdf`, 2005, [Online; accessed 29-August-2017].

[11] G. A. Morton, H. M. Smith, and R. Wasserman, IEEE Transactions on Nuclear Science **14**, 443 (1967).

[12] U. Akgun et al., Journal of Instrumentation **3**, T01001 (2008).

[13] D. Beznosko, Novel multi-pixel silicon photon detectors and applications in T2K, in *Proceedings, Meeting of the Division of the American Physical Society*, 2009.